# ASTRO-H

# INSTRUMENT CALIBRATION REPORT
# SXS DETECTOR GAIN
# ASTH-SXS-CALDB-GAINPIX

Version 0.3

20 December 2016

**ISAS/ GSFC**

**Prepared by:** Megan Eckart, Maurice Leutenegger, F. Scott Porter, Caroline Kilbourne, and the SXS Instrument Team

# **Table of Contents**

# CHANGE RECORD PAGE (1 of 1)

| DOCUMENT TITLE: SXS Detector Gain | | | |
|---|---|---|---|
| ISSUE | DATE | PAGES AFFECTED | DESCRIPTION |
| Version 0.1 | March 2016 | All | First Release |
| Version 0.2 | September 2016 | All | Update based on in-orbit $^{55}$Fe calibration data |
| Version 0.3 | December 2016 | All | Update to 49 mK and 51 mK coefficients. Added discussion of systematic errors on Perseus observations. |

.

# Introduction

## 1.1    Purpose

This document describes the parameterization of the SXS energy gain scale – the relationship between the measured signal and the incident photon energy. Each pixel requires its own gain correction, and the gain must be specified independently for each grade. We derive a non-linear function that describes the gain scale and parameters that describe how the function changes with instrument operating conditions.

The specific nature of any change in operating condition will determine whether the corresponding gain change is linear (a stretch of the gain curve) or non-linear (a change in shape of the gain curve). The gain of each SXS pixel depends linearly on the (small) gain–temperature coefficient of the room temperature amplifiers and has a non-linear scaling with detector temperature.  The detector temperature depends on the CTS temperature setpoint as well as loading on the control thermometers and detector pixels due to nearby structures such as the detector assembly structure (~1.2–1.6K) and the inner vapor cooled shield (IVCS; ~22–35K). These effects tend to change the detector temperatures of all array pixels together. There is also differential radiative loading related to the screening of long wavelength radiation that varies depending on pixel position in the array (i.e., inner pixels are better screened than outer pixels).

We measured the detector gain for each pixel for several detector temperature setpoints in the otherwise nominal ground operating conditions (He mode). These measurements are detailed in Section 5, and the resulting gain parameters are included in the CALDB. From this initial set of gain curves and the measurement of a fiducial line as a function of time during each observation –either using the calibration pixel or pixel-by-pixel– the software pipeline generates an appropriate gain curve that may be used to convert PHA to EPI.

Updates to the gain parameters based on in-orbit measurements are included in the recent releases. The methodology we use to update the ground calibration parameters is described in the sections for CALDB releases 20160510, 20160606, and 20161027, whereas the overall gain calibration methodology and ground calibration measurements are described in the section for CALDB release 20160310.

## 1.2    Scientific Impact

The SXS gain coefficients are used to assign energies for each event via the combination of tasks `sxsgain` and `sxspha2pi`.  The hires coefficients are used in `sxsgain` to calculate a time-dependent effective gain temperature that is used as an input to `sxspha2pi`.  The gain coefficients are used in `sxspha2pi` to construct energy verses PHA curves for each effective temperature and each event grade; the resulting curves are applied to convert PHA to EPI. This gain table is sufficient to provide an accurate energy for primary events of all grades (hires, midres primaries, and lores primaries).

.

Later releases of the software included an option to use a "scale" file in `sxspha2pi`, to scale the PI derived using the ground-calibration gain to the appropriate PI for the on-orbit operating conditions, after applying a drift correction using the calibration pixel (pixel 12). Details of the scale files and when and how they should (or should not) be used are included in the descriptions of CALDB release 20160510 and 20160606.

In addition, for the portion of the on-orbit data taken when the SXS He dewar was coming to equilibrium, a time-dependent gain correction is required. That algorithm is implemented in task `sxsperseus` and uses the ground calibration gain coefficients (`ah_sxs_gainpix_20140101v001.fits`) described in Section 5. The details of the `sxsperseus` task and time-dependent gain correction are described elsewhere; we provide a discussion of the resulting errors in Section 2.5. For the final data release, we determined that it was best to use `sxsperseus` to process observations acquired prior to 00:41 UT on March 4th, 2016, and this is implemented for the final pipeline data release. For earlier data releases, `sxsperseus` was used to analyze a larger set of data: all observations taken before 00:00 UT on March 8th, 2016.

## 2    Release CALDB 20161122

| Filename | Valid data | Release data | CALDB Vrs | Comments |
|---|---|---|---|---|
| ah_sxs_gainpix_20140101v003.fits | 2016-03-04 00:41 UT | 20161122 | 005 | Original ASCII files: gain_49mK_SXS_v3.0.txt gain_51mK_SXS_v3.0.txt<br><br>SHPTEMPL=2015-03-10 |

**Approach:** For CALDB 20160606 we provided updated 50mK gain curves for all pixels and all event grades based on the on-orbit filter wheel (FW) [55]Fe dataset, but we did not update the 49 mK or 51 mK gain curves. In this release we provide updated 49 mK and 51 mK gain curves, stretched linearly from the ground-calibration curves.

### 2.1    Data Description

The data used for these updates were obtained using the filter wheel [55]Fe source on March 19th, 2016, under nominal on-orbit operating conditions. The data and dewar operating conditions are described in Section 3.1.

### 2.2    Data Analysis

In Section 3.2 we describe the method by which we redefined the final SXS steady-state temperature to be 50 mK by stretching the 50 mK gain curves, and report that we did not similarly stretch the 49 and 51 mK gain curves for CALDB 20160606 since, for the period of interest, the temporal corrections to each pixel's gain curves are based on very small relative changes in the measured gain of the calibration pixel, which stays close to an effective temperature of 50 mK.

.

However, by stretching the 50 mK curves but not the 49 or 51 mK curves, we introduced a small asymmetry, where the stretched 50 mK gain curves end up closer to the 51 mK curves and farther from the 49 mK curves. For some pixels the stretch parameters are large enough that the asymmetry is of order 10% (where the offset of the MnKα complex in the FW data would imply an effective temperature of 50.1 mK using the pre-launch gain scales). The asymmetry can cause, at the most, a gain error of ~0.3 eV at 6 keV.

In this release we remove the small asymmetry by stretching each 49 and 51mK curve (per pixel and per event grade) by the same factors used to stretch the 50 mK curves.

In addition, we further investigated the best date to stop using the `sxsperseus` time-dependent correction and instead use these updated gain curves We find that the best stop time is 00:41 UT on March 4th, 2016, approximately four days earlier than in the previous CALDB release.

## 2.3  Results

We update the 49 mK and 51 mK polynomial gain coefficients for each pixel and each event grade. The 50 mK coefficients remain the same as supplied in CALDB 20160606. The validity date is 00:41 UT on March 4th, 2016.

## 2.4  Changes from last release

The gain coefficients for 49 mK and 51 mK effective temperatures have been updated to be consistent with the on-orbit data. This eliminates a small asymmetry at the 10% level that we introduced in CALDB release 20160606, which caused, at the most, a gain error of ~0.3 eV at 6 keV.

The change in the stop time for using `sxsperseus` changes the treatment of SEQ_IDs 100040030, 100040040, 100040050, and 100040060.  This results in no significant change to the energy scale for 100040060, but the energy scale for the other three, in aggregate, results in a 1.5 eV increase at 6.5 keV.  Because these observations, and 100040020, contain largely overlapping regions of Perseus, we can see that the change brings 100040030-50 into better agreement with 100040060, but there is now a discrepancy between them and100040020.

## 2.5  Errors

In previous releases, we did not provide an estimate of systematic errors.  We do so here.  The estimated errors depend on the time of the observation and the energy.

After 22:57 UT on March 6th, 2016 (starting with 100040060), SXS gains have stopped trending monotonically, and from this point they follow a pattern based on the ADR recycling.  Based on the errors at the Mn Kβ line in the calibration data taken with the FW $^{55}$Fe source, we estimate a systematic uncertainty of 0.5 eV from about 5 – 7 keV, with it being closer to 0.2 eV right at 5.9 keV.  Errors will increase above and below this range – above because of the use of linear rescaling of the gain function and below due to the lack of calibration in the flight system below 4 keV.  From instrumental lines, we know that collectively there is an error of 2-3 eV around 2 keV, but the statistics do not permit evaluation by pixel.

For the interval between 00:41 UT on March 4$^{th}$, 2016 and 22:57 UT on March 6$^{th}$, 2016, the temperatures are still equilibrating, but `sxsperseus` was determined to introduce more error than it corrects, and thus it is not applied. However, the energy scale should be considered to have larger systematic error than after equilibration. We recommend using a systematic error of 1 eV around 6 keV, increasing below 4 and above 7 keV; comparison to overlapping regions of 100040060 should also be made to check systematics.

`sxsperseus` was used to correct 100040020. Uncertainties in the fits extrapolating the fiducial measurement to 100040020 estimate that `sxsperseus` may introduce up to a 1.5 eV systematic error at 6.7 keV. Comparisons to 100040030-50, which is largely in equilibrium, show a 1.5 eV difference for the same target region. Thus we recommend adopting a 1.5 eV systematic error for this sequence around 6 keV, again increasing below 4 and above 7 keV.

The lack of overlap of the 100040010 pointing with subsequent Perseus pointings leaves that data set completely without a reference. Again, uncertainties in the extrapolations used by `sxsperseus` estimate a systematic error between 2 and 3 eV, but with no independent method of confirmation. We recommend caution when using absolute energy scales in sequence 100040010. However, the systematic error may be estimated by a careful comparison of 100040010 and 10040030-50 in adjacent spatial areas and comparing the He-like Fe line displacement to the maximum shear allowed by measurements of the velocity broadening in adjacent pixels in the two observations. The estimated error in the adjacent regions is likely representative of the rest of 10040010. Other attempts to assess the systematics in that very first observation are planned.

## 3  Release CALDB 20160606

| Filename | Valid data | Release data | CALDB Vrs | Comments |
|---|---|---|---|---|
| ah_sxs_gainpix_20140101v002.fits | 2016-03-08 | 20160606 | 003 | Original ASCII file: gain_50mK_SXS_v3.0.txt  SHPTEMPL=2015-03-10 |
| ah_sxs_scale_20140101v002.fits | 2016-03-08 | 20160606 | 003 | Original ASCII file: gain_stretch_20160526_wGroundCalGain.txt  SHPTEMPL=2015-03-10 |

**Approach:** We provide updated 50mK gain curves for all pixels and all event grades based on the on-orbit filter wheel (FW) $^{55}$Fe dataset. We stretch each gain curve linearly using the measured on-orbit offset in gain at Mn K$\alpha$. There will be an error associated with this method of at most a couple of eV away from the 5.9 keV pinning point. We do not supply new 49mK or 51mK gain curves.

Also, we supply a 'scale' factor for each pixel and each event grade that is compatible with the pre-launch 50mK CALDB file (release 20160310). See Sections 3.2–3.4 for details about when and how to use this scale file.

## 3.1    Data Description

The data used for this update were obtained using the filter wheel $^{55}$Fe source on March 19$^{th}$, 2016, under nominal on-orbit operating conditions. The heatsink temperature was 50 mK and the helium tank had reached its on-orbit equilibrium temperature of 1.1 K. Table 1 lists relevant instrument parameters; it may be compared to Table 3, which summarizes these same parameters during ground calibration.

| PSP Parameters | | Comments |
|---|---|---|
| Thresholds | 120 for all pixels | PULSE_THRES and NOISE_THRES are set to these values. |
| Templates | SHPTEMPL=2015-03-10 | |
| Average pulse scale | pix 0-35 = 144000 | PSP parameter PHA_AVGPULSE |
| Software Version | 0x150615 | |
| | | |
| **XBOX Parameters** | | |
| Detector Bias Setpoint | 1.60784V | 0x0052 in hex |
| Detector Bias Readback | 1a=1.581V, 1b=1.584V, 2a=1.582V, 2b=1.588V | |
| | | |
| **ADRC Parameters and Relevant Temperatures** | | |
| CTS Temperature Setpoint | 50 mK | |
| Control Thermometer | CT0 Sensor0 | |
| DA Temperature | 1.125–1.132 K | He mode operation |
| He Tank Temperature | 1.116–1.122 K | on-orbit equilibrium temperature |
| IVCS Temperature | 23.1–23.2 K | |

**Table 1 Selected instrument parameters during SXS on-orbit filter wheel $^{55}$Fe measurements.**

## 3.2    Data Analysis

We analyzed the data using software and CALDB versions 1. We fit the MnKα spectra using XRSGSE version 10.7.6b1.

Figure 1 provides an example to help illustrate our approach. On orbit, the PHA of the calibration pixel is slightly larger than it was when we took the ground calibration data. Thus, when running sxsgain and drift correcting using the calibration pixel, the calculated effective temperature is slightly less than 50 mK.

.
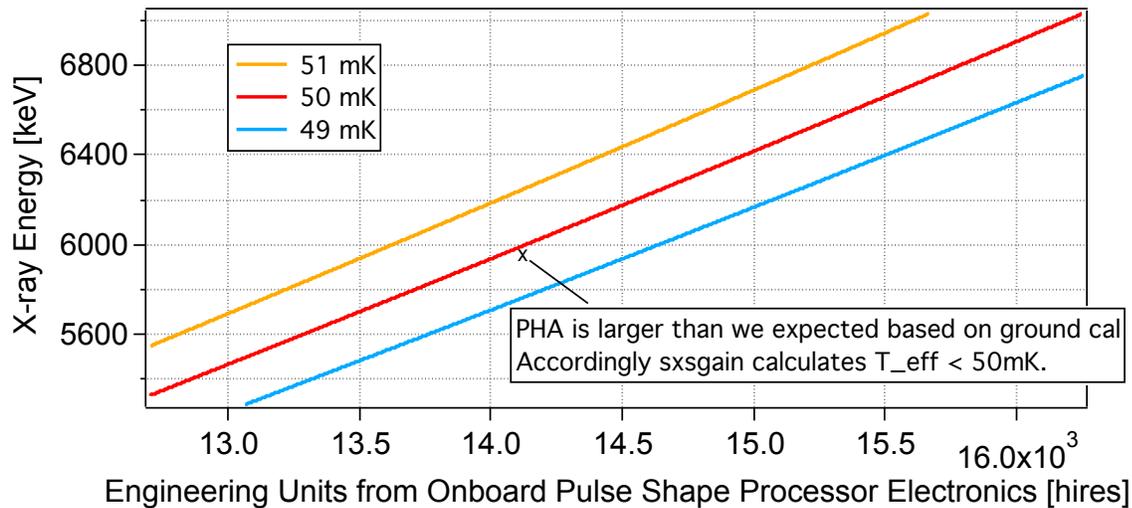
**Figure 1 Plot of the original ground calibration gain curves at the three heatsink temperatures, and an "x" showing an example of where the on-orbit MnKα peak (5.9 keV) lies compared to these curves.**

To correct this difference in the calibration pixel gain and define a new 50mK gain, as illustrated in Figure 2, we analyzed the calibration pixel data forcing the effective temperature to 50 mK; i.e., we forced the pipeline to use the original 50.0 mK ground calibration curve. We found an apparent energy shift of 1.39 eV using hires data on the calibration pixel.
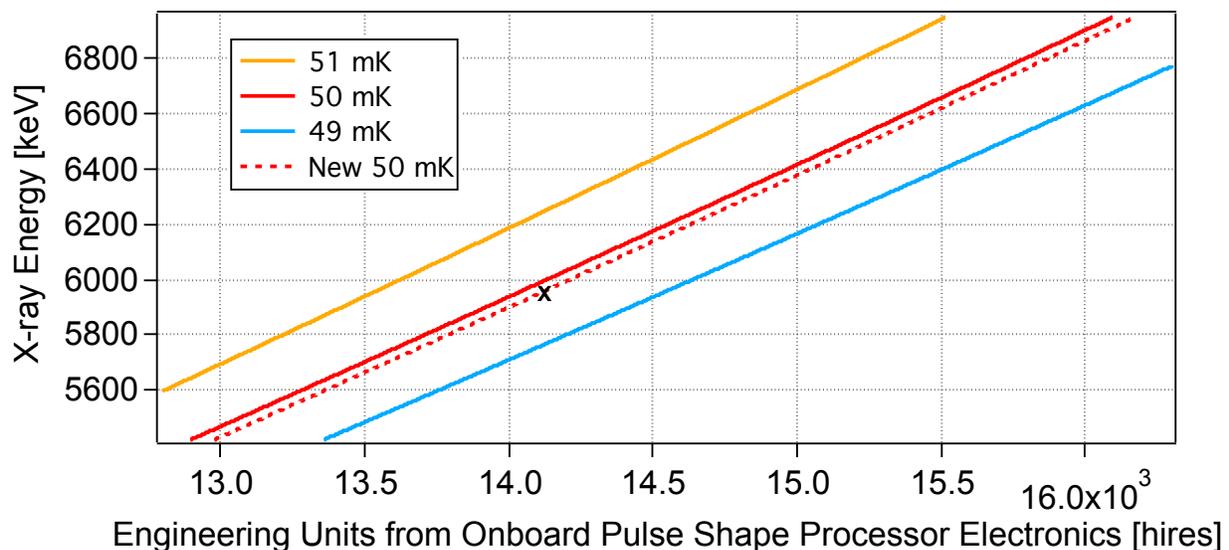


**Figure 2 Using the centroid of the MnKα complex, we derive new 50 mK gain curves for each pixel, as indicated by the dashed line.**

Next we calculated the apparent energy offsets for all pixels and all event grades with respect to the hires events on the calibration pixel, using data where the standard drift correction was applied. We fit the MnKα spectrum for each pixel using XRSGSE version 10.7.6b1, and

recorded the centroid of the line complex. We performed fits separately for each event grade. There were ample hires counts but few midres counts on all but the calibration pixel, which led to larger error bars on the midres energy shifts of the main array pixels. For lores we used the LO_RES_PHA for all events, as described in Section 5.1. The resulting shifts are presented in Figure 4.

The energy offsets on the array pixels were larger than seen for the calibration pixel, equivalent to an ~0.1 mK change in effective temperature, and the pattern of offset on the array was unlike the usual differential loading pattern seen on the ground. But, we found that the relative gain drift pattern of the individual pixels does follow the standard pattern of differential loading as observed in ground testing. Thus, there appears to have been an overall static gain change experienced upon operation in orbit, for example due to amplifier gains. The reason for this shift in gain is not understood and remains an active area of investigation.

Because we lack calibration lines on the array at any other time besides the FW measurement, the array pixel gains cannot be self-corrected. Thus we align the array-pixel gains using the FW $^{55}$Fe data, so that we can use changes in the calibration pixel gain to track and correct small time-dependent gains of all pixels. We use the measured gain offsets at Mn K$\alpha$ to calculate to a linear scaling factor to stretch the gain scales appropriate for ground operating conditions, and, for comparison, we also calculate gain scales using a non-linear correction, where we assume the offset at MnK$\alpha$ indicates a change in effective detector temperature. We tested both sets of gain scales and compared the resulting offsets at MnK$\beta$ (6.4 keV) in the FW data. Both methods resulted in a small systematic gain error at Mn K$\beta$ and it is likely that the appropriate solution is some combination of the two methods. Given this ambiguity and the limited on-orbit calibration data, we proceed using the linearly stretched curves. Using this method, as opposed to a non-linear function (see Ref. [2]), will introduce an error of at most a couple of eV away from the pinning point.
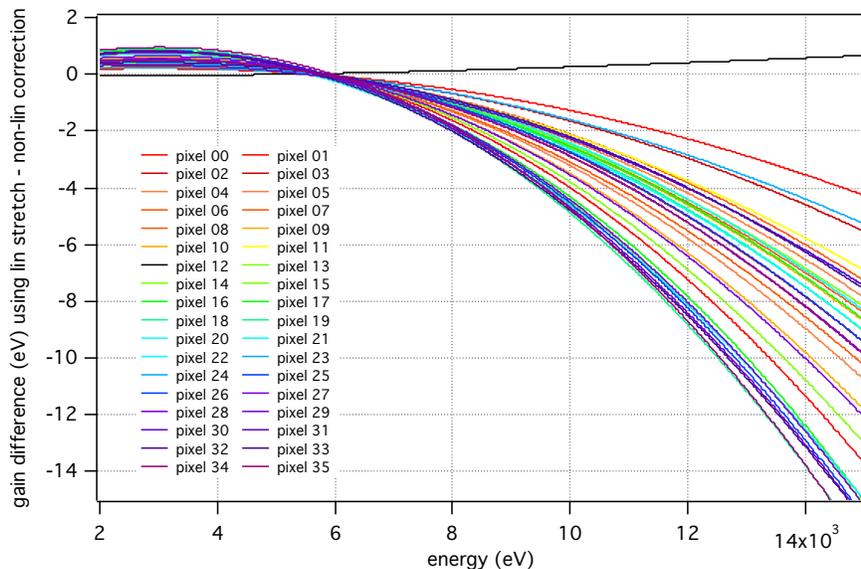


**Figure 3 Difference in hires gain curve resulting from different methods of correcting the the ground-calibration gain curves to match on-orbit conditions: a linear stretch or a non-linear correction, each based on the apparent energy shift at MnK$\alpha$ in the on-orbit FW $^{55}$Fe dataset.**

.

We do not correct the coefficients for 49 and 51 mK because we are only able to scale the temporal gain changes relative the calibration pixel gain, which remains very close to an effective temperature of 50 mK for the period of interest (when the He dewar is in its on-orbit equilibrium state).

Using midres events, the error bars on the individual MnKα line centroids are large. The average offset between midres events and hires events on each pixel is –0.9 eV. For the calibration pixel, where there are ample midres counts, the offset at MnKα is –0.83 eV (1–0.83/5898 = 0.999859) and the offset at MnKβ is –0.93 eV (1–0.93/6490 = 0.999857), from which we conclude that this midres-to-hires offset can be treated as an additional scaling term.

Using the measured offsets we calculate a stretch term for the hires data for each pixel, and an additional stretch term for midres and lores gains to account for the offsets with-respect-to the hires data. Because the error bars are large on the individual midres fits, we use an average correction term for all pixels; for lores we employ a per-pixel correction. These correction fractions are enumerated below.

We apply the stretch terms to the gain curves derived from the ground calibration data, and then re-fit the curves to derive updated polynomial coefficients.
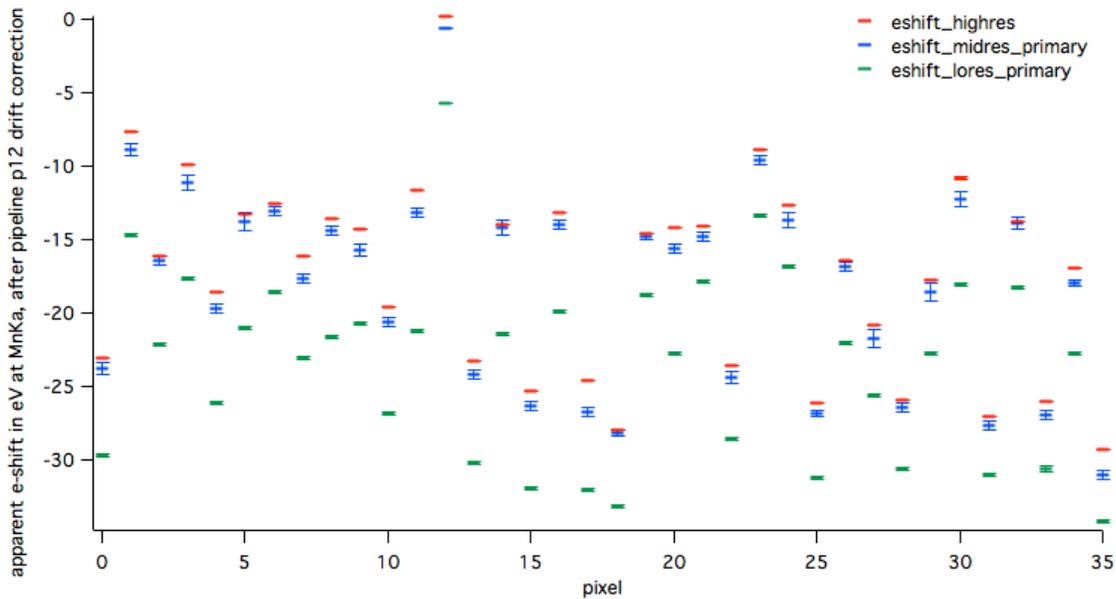


**Figure 4 Apparent energy shift at MnKα, for each pixel and each event grade, from the on-orbit FW $^{55}$Fe dataset. The data were processed using the pipeline using "fit" method to drift correct using the calibration pixel in sxspha2pi, and the gain scales in CALDB 20160310.**

Stretch terms used to stretch the gain curves and derive new polynomial gain coefficients:

Hires: stretch per pixel

$$f\_hi_i = 1 - ((eshift\_hi_i - eshift\_hi_{12}) + eshift\_hi_{12\_using\_50mK\_gain\_for\_drift})/5895 \text{ eV}$$
$$= 1 - ((eshift\_hi_i - 0.185 \text{ eV}) + 1.39 \text{ eV})/5895 \text{ eV}$$

*Note: the parameter labeled eshift_hi$_{12}$ refers to an 0.185 eV energy shift at MnKa measured in the hires data on the calibration pixel, despite having performed the drift correction on the very same line. We assume that this 0.185 eV offset is an artifact due to a small bug in the pipeline processing, and we subtract it here, as shown above. This offset is under investigation.*

Midres: apply same stretch as for hires per pixel plus an additional stretch to all pixels

$$f\_mid_i = f\_hi_i * (1 - (<eshift\_mid_i - eshift\_hi_i>)/5895 \text{ eV})$$
$$= f\_hi_i * (1 + 0.9 \text{ eV}/5895 \text{ eV}) = f\_hi_i * 1.0001527$$

Lores: apply same stretch as for hires per pixel plus an additional per pixel stretch

$$f\_lo_i = f\_hi_i * (1 - (eshift\_lo_i - eshift\_hi_i)/5895 \text{ eV})$$

To calculate the new gain coefficients using these scaling fractions, we calculate the energy vs. PHA curve based on the original 50 mK CALDB parameters (v001.fits, described in Section 5), multiply the curve by f_grade$_i$, and re-fit the curve for new gain coefficients.

In addition to new 50mK gain curves, we provide a scale file that can be used in conjunction with the ground 50mK gain curve (v001.fits, described in Section 5). In this case the ground 50 mK gain is used for both `sxsdrift` and `sxspha2pi`, but with `scalepi=yes` in `sxspha2pi`, so that $E_{corrected} = E_{ground\_gain} * g\_grade_i$, where $E_{ground\_gain}$ has been generated by drift correcting using the calibration pixel and g_grade$_i$ is a per-pixel, per event-grade stretch term. We calculate g_grade$_i$ in the same way as the fractions described above, except the 1.39 eV term is not included in g_hi$_i$, as compared to f_hi$_i$. (So, for example, pixel 12 hires stretch term is 1.0.)

### 3.3    Results
We update the 50 mK polynomial gain coefficients for each pixel and each event grade, so that the gain parameters are consistent with the on-orbit instrument conditions. We provide a scale file with four columns: pixel number, hires scale factor, midres scale factor, and lores scale factor.

### 3.4    Changes from last release
The gain coefficients have been updated to be consistent with the on-orbit data, appropriate for data taken once the SXS He dewar came into thermal equilibrium. We also supply an update to the scale file introduced in CALDB 20160510 that was only appropriate for hires events; the new version includes scaling terms for each event grade. Note that the scale file should never be used with the updated gain coefficients; it is only appropriate for use with the original gain curves (v001.fits, described in Section 5), and after applying a drift correction using the calibration pixel.

# 4  Release CALDB 20160510

| Filename | Valid data | Release data | CALDB Vrs | Comments |
|---|---|---|---|---|
| ah_sxs_scale_20140101v001.fits | 2014-01-01 | 20160510 | 002 | SHPTEMPL=2015-03-10 |

The scale file released with CALDB 20160510 was intended for initial analysis of on-orbit data, to be superseded when the full version of the on-orbit gain parameters were ready for release.

## 4.1  Data Description

The data supplied in this update were obtained using the filter wheel $^{55}$Fe source on March 19$^{th}$, 2016, under nominal operating conditions. The heatsink temperature was 50 mK and the helium tank had reached its on-orbit equilibrium temperature of 1.1 K. Table 1 lists relevant instrument parameters; it may be compared to Table 3, which summarizes these same parameters during ground calibration.

## 4.2  Data Analysis

We analyzed the data using software and CALDB versions 1, and performed drift correction using the calibration pixel. We fit the resulting MnK$\alpha$ spectrum for each pixel using XRSGSE version 10.7.6b1, and recorded the centroid of the line complex, allowing us to derive a gain offset for each pixel. For this initial scale file, the measurements were derived using hires events only. These hires shifts are presented in Section 3.1, Figure 4. The change in gain (from the ground measurements) is small and we assume that it is linear, so that these offsets may be converted to a linear scaling factor to correct the event energy.

## 4.3  Results

We provide scaling parameters that may be used to correct the pulse height (PI) for each pixel. The CALDB file contains two columns: pixel number (0-35) and scaling factor. These are to be used in conjunction with the polynomial coefficients derived from the ground calibration data, described in release 20160310. The gain was close to that measured on the ground, and these hires scaling factors lie in the range $0.99996 < f < 1.005$ (within 0.5% of the ground measurements at 5.9 keV).

## 4.4  Changes from last release

This scaling file was used as a rough first update to the gain parameters based on on-orbit measurements. It is valid for data acquired on or after March 8$^{th}$, 2016, when the SXS He dewar had come to its equilibrium state. It was intended as a temporary file, and was soon thereafter superseded by the files released in CALDB 20160606.

.

# 5    Release CALDB 20160310

| Filename | Valid data | Release data | CALDB Vrs | Comments |
|---|---|---|---|---|
| ah_sxs_gainpix_20140101v001.fits | 2014-01-01 | 20160310 | 001 | Original ASCII files: gain_49mK_SXS_v2.0.txt gain_50mK_SXS_v2.0.txt gain_51mK_SXS_v2.0.txt  SHPTEMPL=2015-03-10 |

## 5.1    Data Description

The calibration measurements of the SXS detector gain were performed in March 2015 during SXS instrument-level testing at Tsukuba Space Center (TKSC) using the flight version of the electronics boxes (XBOX, ADRC). The SXS dewar was in its final flight configuration, following the installation of the isolators between the dewar and the cryocoolers.

We used a Rotating Target X-ray Source (RTS) positioned above the dewar to provide x-ray lines at known energies from 4.5–13.5 keV. Figure 5 presents a photo of the experimental setup. Calibration at low x-ray energies was not possible at TKSC due to the presence of the gate valve's beryllium window.

The RTS consists of a bright x-ray continuum source (TruFocus model 5110 with tungsten target) that illuminates targets mounted on a rotating wheel. Fluorescence from the targets provides x-ray line emission directed to the instrument aperture. The targets are typically single crystal and are adjusted to steer Bragg-reflected photons away from the detector. For the case of the gain measurements we used the following targets in the eight slots: 0) Fe, 1) KBr, 2) Cu, 3) GaAs, 4) Co, 5) Cr, 6) Mn, 7) $TiO_2$. The x-ray source settings were HV = 20kV and $I_{emission}$ = 30µA (for 49mK and 50mK hires data) or = 40µA (for 50mK midres and 51mK hires data) and the dwell time at each target was one minute, providing approximately 1 ct/s/pixel.

The data were acquired using the Pulse Shape Processor (PSP). The PSP calculates the PHA of each event onboard.  For hires and midres grades the events are optimally filtered and the result is assigned to the PHA column of the event file. Please see Szymkowiak et al. (1993) [4] and Boyce et al. (1999) [1] for background on optimal filtering for microcalorimeters. Hires events are calculated using a 1024-sample optimal filter while midres events are calculated using a 256-sample optimal filter. Each pixel has a hires and midres optimal filter template stored onboard, and a given set of the 72 filter templates are identified by the SHPTEMPL keyword. The current optimal filter templates were calculated during the calibration phase in March 2015 and assigned SHPTEMPL = 2015-03-10.

.
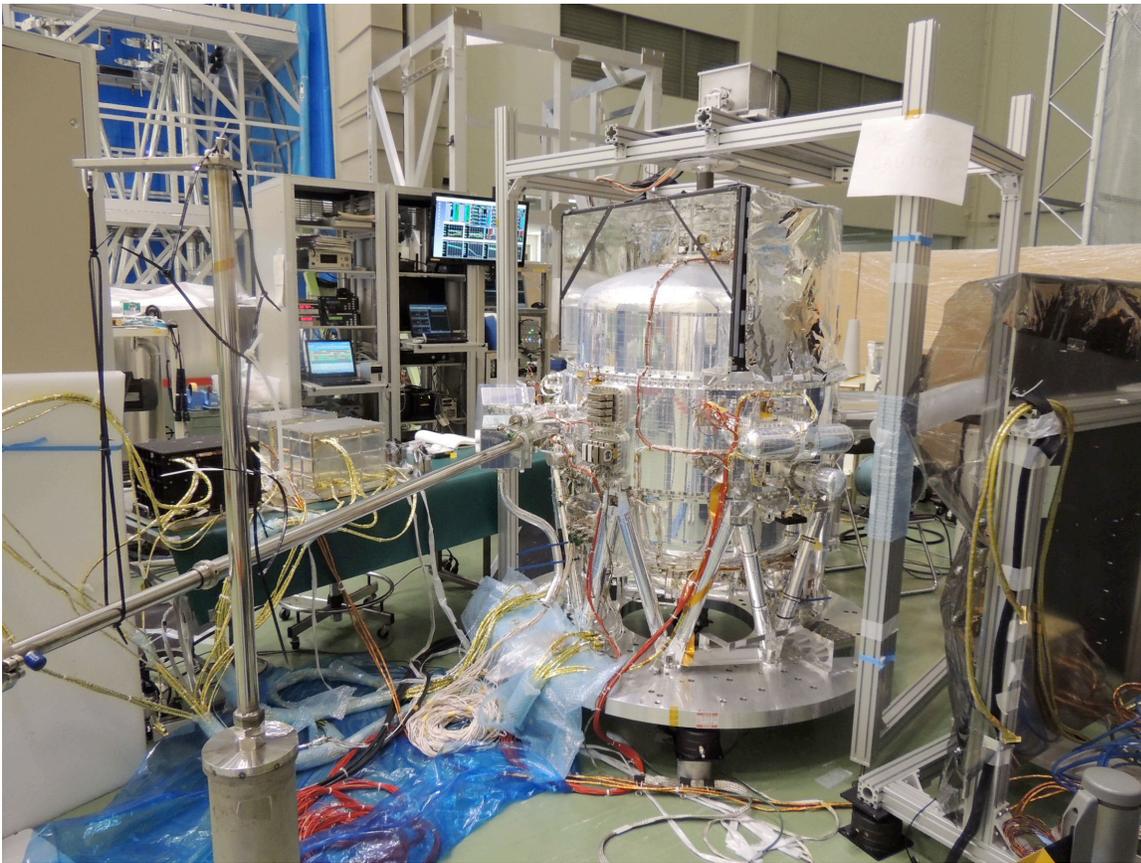
**Figure 5 Rotating Target X-ray Source (RTS) mounted above the flight instrument in March 2015.**

Lores events are not optimally filtered in the PSP; instead their pulse height is given by maximum ADC value in the sample record (after subtracting the baseline value of the sample). In fact, this 'lores pulse height' is calculated not just for lores events but for events of all grades. For hires and midres events the result it is placed in the LO_RES_PH column whereas for lores events it fills both the LO_RES_PH and the PHA columns. Because the LO_RES_PHA is telemetered for all event grades, we acquire simultaneous lores gain scale information during experiments aimed at calibrating hires or midres event grades.

To acquire spectra for the hires and lores gain scales we operate the PSP in its normal mode. For the hires gain scale we derive curves by relating the PHA (ADC units) to energy (eV) using hires events. For the lores gain scale we use all primary events (hires, midres primaries, and lores primaries) but relate the LO_RES_PHA (ADC units) to energy (eV).

To obtain a sufficient number of midres events in a reasonable exposure time, both in the case of our relatively low count-rate energy scale calibration setup at TKSC and for appropriate celestial sources, we operate the PSP in forced midres mode. In this mode hires-graded events are processed as if they were midres (using the 256-sample optimal filter template) so that both hires and midres events may be combined to measure a midres gain scale by relating the PHA (ADC units) to energy (eV).

.

Based on analyses of gain curves measured over a wide span of instrument operating conditions, including in cryogen free mode, we find that we may treat all gain variations as equivalent to changes in detector temperature. As a result, we use the following approach. For each event grade we provide gain curves at three bath temperatures. The intention is that the resulting gain curves will envelope the gain curves we are apt to encounter during the mission lifetime. These curves are then used in the software pipeline, in conjunction with a measured fiducial line, to construct a gain curve appropriate for the instantaneous operating conditions of the instrument. See Porter et al. (2015) [2] for details about this non-linear drift correction approach. In nominal operating conditions on the ground the instrument gain is typically very close to the 50mK gain curve and the gain correction applied by the pipeline is approximately a small linear stretch to the 50 mK gain curve.

Each gain calibration experiment was recorded as an Igor Pro experiment using the XRSGSE software suite version 10.5.1. Table 2 provides the experiment names as well as the start and stop times of each exposure, while Table 3 presents selected operating parameters for onboard SXS electronics boxes (PSP, XBOX, and ADRC) and relevant operating temperatures.

| Temp [mK] | Hires/Lores experiment name | Hires/Lores Start Time [UT] | Hires/Lores Stop Time [UT] | Midres experiment name | Midres Start Time [UT] | Midres Stop Time [UT] |
|---|---|---|---|---|---|---|
| 49.0 | 15-03-11.07.48.06Z | 3/11/2015 08:03 | 3/11/2015 16:01 | n/a | n/a | n/a |
| 50.0 | 15-03-11.16.24.16Z | 3/11/2015 16:25 | 3/12/2015 04:38 | 15-03-12.13.56.25Z | 3/12/2015 13:59 | 3/13/2015 01:08 |
| 51.0 | 15-03-13.01.40.55Z | 3/13/2015 01:41 | 3/13/2015 09:40 | n/a | n/a | n/a |

**Table 2 Experiment files and start/stop times for the gain calibration measurements.** The lores gain parameters are derived using the LOW_RES_PH of all primary events; a separate experiment is not required. For the midres experiment the PSP was in forced midres mode.

.

| PSP Parameters | | Comments |
|---|---|---|
| Thresholds | pix 10,15-17,21-22,25,28-31,34 = 24; pix 0-7,11-12,14,19,24,32-33,35 = 25; pix 13,18,23 = 26; pix 9 = 28; pix 8 = 32; pix 20 = 29; pix 27 = 40; pix 26 = 62 | PULSE_THRES and NOISE_THRES are set to these values. A threshold of 25 corresponds to ~34 eV. |
| Templates | SHPTEMPL=2015-03-10 | |
| Average pulse scale | pix 0-35 = 144000 | PSP parameter PHA_AVGPULSE |
| Software Version | 0x150310 | |
| | | |
| XBOX Parameters | | |
| Detector Bias Setpoint | 1.60784V | 0x0052 in hex |
| Detector Bias Readback | 1a=1.582V, 1b=1.585V, 2a=1.583V, 2b=1.588V | |
| | | |
| ADRC Parameters and Relevant Temperatures | | |
| CTS Temperature Setpoint | 49.0 / 50.0 / 51.0 mK | |
| Control Thermometer | CT0 Sensor0 | |
| DA Temperature | 1.220–1.232 K | He mode operation |
| He Tank Temperature | 1.216–1.227 K | |
| IVCS Temperature | 26.5–26.9 K | |

**Table 3 Selected instrument parameters during SXS gain ground calibration.**


## 5.2   Data Analysis

**Overview**

For each experiment we follow a standard procedure to determine the detector gain curve. The following prescription is performed independently for each of the array pixels. First, we apply a linear drift correction to the data, if necessary, to remove very small changes in effective detector temperature over the course of the exposure. Next, we histogram the events with bin width of ~1 ADC unit (~0.5 eV). We then fit each of the x-ray line complexes to determine a set of PHA–energy pairs and associated error estimates. Finally, we fit these data to the fourth-order polynomial given in Eq (1):

$$E \text{ [eV]} = c1*PHA + c2*PHA^2 + c3*PHA^3 + c4*PHA^4. \qquad \textbf{Eq. ( 1 )}$$

One exception is the calibration pixel (pixel 12). Since it only receives photons from the collimated [55]Fe source, not from the instrument aperture, we must derive its gain scale from fits to two only line complexes (Mn Kα and Kβ). Therefore, we constrain the fit function to a second order polynomial (c3=c4=0).

.

To allow for greater flexibility in the CALDB, in addition to terms c1–c4, we also include the option of a linear offset term (c0) and a fifth order term (c5); however, the current gain files have each of these terms set to zero for all pixels.

**Hires**

For each of the three heatsink temperatures we make spectra for each pixel using hires events. We fit the following line complexes: Ti Kα, Cr Kα, Mn Kα, Fe Kα, Co Kα, Cu Kα, Ga Kα, As Kα, and Br Kα.

**Midres**

We acquired data at 50 mK in forced midres mode, in which both hires and midres events are processed with the 256-sample (midres) optimal filter template (as described in Section 5.1), allowing much more efficient data collection for midres-processed pulses. We use the same set of x-ray line complexes as described for the hires gain.

A linear stretch (~0.9998) has been applied to the resulting 50 mK midres gain scales to correct for a slight difference in the effective temperature during the forced midres exposure as compared to the 50 mK hires exposure.

We did not have time to acquire data in forced midres mode at 49mK and 51mK prior to delivery to the spacecraft. Instead, we calculate the gain components by scaling the 50 mK midres gain curve by the ratio of the 49 mK (or 51 mK) hires gain curve to the 50 mK hires gain curve, and then fitting a 4th order polynomial to the resulting curve. We tested the efficacy of this approach by evaluating the (low-statistics) midres primary lines obtained during the 49/51 mK hires experiments and found that the results give errors of less than 5 eV at 49mK and less than 10 eV at 51 mK. These are deemed acceptable for nominal cryogen mode observations since we operate very close to the 50 mK gain curves given in the CALDB.

**Lores**

We used the LO_RES_PHA of primary events of all grades, as described in Section 5.1, and fit the same set of lines to determine the gain curves at each temperature. Since the lores data were acquired simultaneously with the hires data, the reference effective temperature for each dataset was by definition the same and did not require additional processing (as in the case of the midres data).

## 5.3 Results

The resulting gain parameters for each pixel and each event grade are given in the CALDB file. The following plots give examples of the gain curves, for reference. The residuals on the fits are within +/- 0.5 eV for the hires and midres gain curves and +/- 2.5 eV for the lores gain curves over the range 4.5–12 keV.
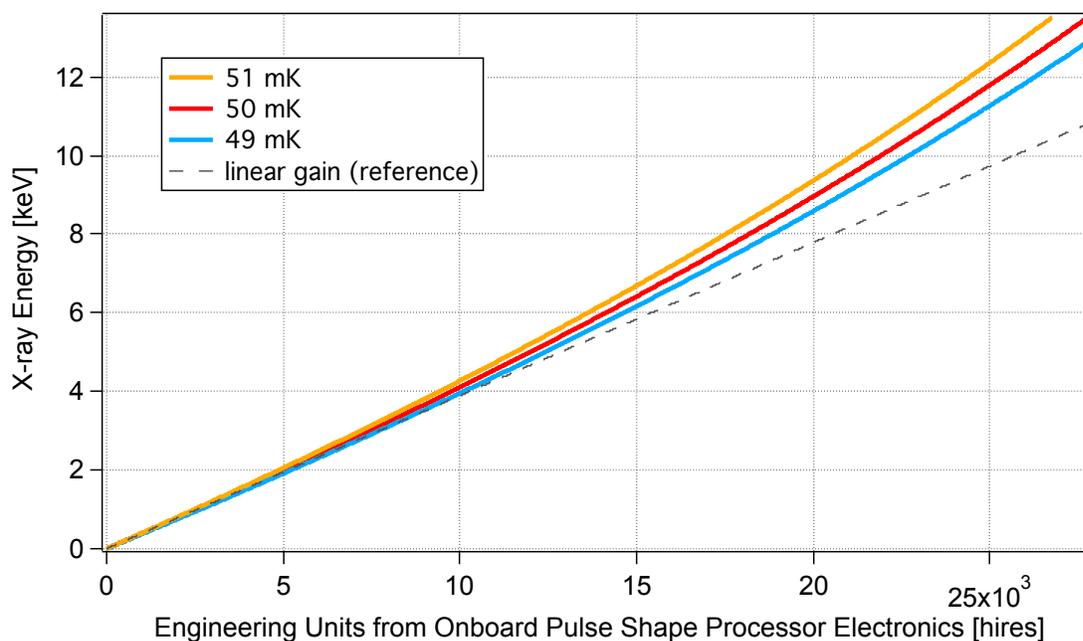


**Figure 6 Hires gain scales for pixel 0 calculated using the polynomial coefficients given in the CALDB file.** The 49 mK and 51 mK gain scales bound the gain conditions we expect to encounter on-orbit.
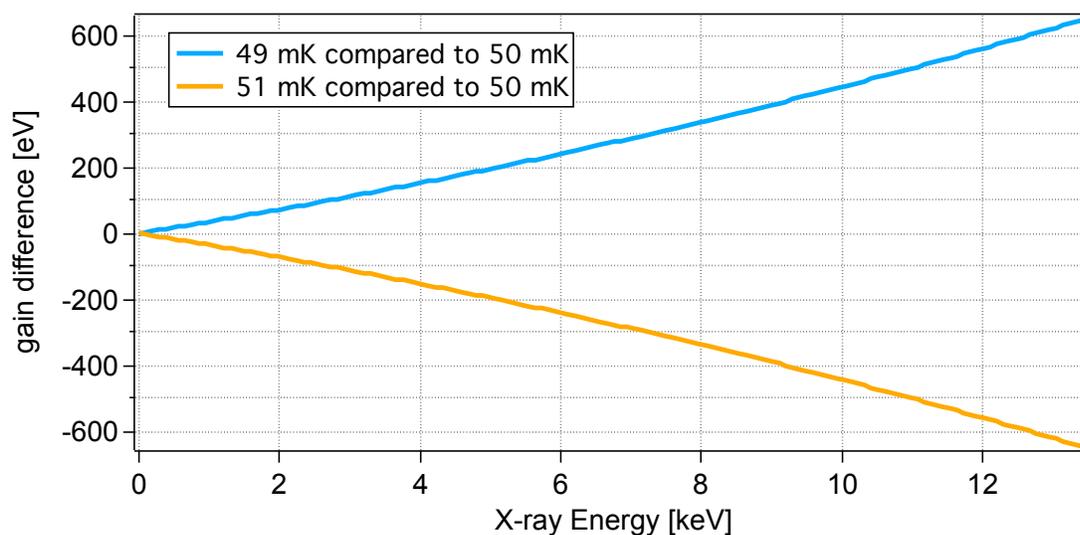


**Figure 7  This plot highlights the difference in gain between the hires gain scales at different heatsink temperatures.**

.

## 5.4    Final Remarks

During initial in-flight calibration we plan to check the SXS gain using a combination of on-board sources and celestial sources for a set of operating conditions (49mK, 50mK, 51mK; and in forced midres mode at each temperature). Our aim is to have parameterized the gain in such a way that even if operating conditions change slightly, the change in gain is wholly described by a change in effective temperature, and will not require new CALDB files. However, we expect that the addition of low-energy lines in the calibration measurements as well as the forced midres data at 49 and 51 mK will produce changes significant enough to warrant a new release.

If at any time the optimal filter templates (keyword SHPTMPL) for one or more pixel are changed on-orbit then the gain calibration for hires and midres event grades will need to be modified accordingly. While we intend to use these same optimal filter templates for the entirety of the mission so as not to invalidate the ground calibration, if the on-orbit noise conditions change substantially then we will consider changing the optimal filter templates.

In addition to the data used to create the current CALDB gain curves, we also performed similar measurements in cryogen free mode with several combinations of CTS control temperature, detector assembly structure control temperature, and IVCS temperature. These measurements are not required for the CALDB, but were essential in verifying our approach and confirming that the 49mK/51mK He-mode data envelope the gain conditions we expect during cryogen free mode. We also acquired ground calibration data at TKSC over an extended energy bandpass – to energies of 25 keV. These data are not included in the current release of the CALDB, but may be incorporated at a later stage if deemed necessary. Figure 8 illustrates the magnitude of gain errors that will arise above ~12 keV due to our not including the high energy measurements in the CALDB gain parameters.
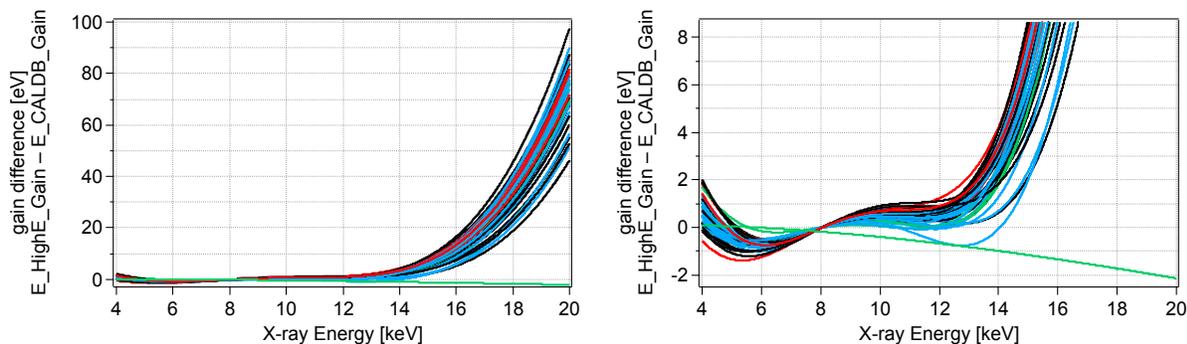


**Figure 8  (Left) The difference in derived event energy using the high-energy ("HighE") gain coefficients compared to the gain coefficients in the CALDB for the 36 SXS pixels.  The CALDB gain coefficients will underestimate energies by 45–100 eV at 20 keV. The green curve is the calibration pixel.**
**(Right) Zoom highlighting that the gain scales agree to within ~ ± 1 eV to 13 keV.**

Finally, we re-emphasize that these gain curves will only provide precise energies for primary events. An additional correction is required to recover the energy of secondaries. A CALDB file

exists to aid in correcting midres secondaries (CALDB filename = `ah_sxs_secpulse_20140101v00N.fits`), and will be described elsewhere.

## 6   References

[1] K.R. Boyce, M.D. Audley, R.G. Baker, J.J. Dumonthier, R. Fujimoto, K.C. Gendreau, Y. Ishisaki, R.L. Kelley, C.K. Stahle, A.E. Szymkowiak, and G.E. Winkert. "Design and performance of the ASTRO-E/XRS signal processing system," *Proc. SPIE,* **3765,** 741-750 (1999).

[2] F.S. Porter, M.P. Chiao, M.E. Eckart, R. Fujimoto, Y. Ishisaki, R.L. Kelley, C.A. Kilbourne, M.A. Leutenegger, D. McCammon, K. Mitsuda, M. Sawada, A.E. Szymkowiak, Y. Takei, M. Tashiro, M. Tsujimoto, T. Watanabe, and S. Yamada. "Temporal Gain Corrections for X-ray Calorimeter Spectrometers," *Journal of Low Temperature Physics,* p1-7 (2016). DOI: 10.1007/s10909-016-1503-2.

[3] A.E. Szymkowiak, R.L. Kelley, S.H. Moseley, and C.K. Stahle. "Signal processing for microcalorimeters," *JLTP,* **93,** 281-285 (1993).